UNIVERSITY OF CALIFORNIA
RIVERSIDE

Purkinje Neuron Dysfunction in a Mouse Model of Multiple Sclerosis

A Thesis submitted in partial satisfaction
of the requirements for the degree of

Master of Science

in

Biomedical Sciences

by

Marvellous Ehrunmwunse Osunde

June 2022

Thesis Committee:

Dr. Seema Tiwari-Woodruff, Chairperson
Dr. Edward Zagha
Dr. Brandon Brown

The Thesis of Marvellous Erhunmwunse Osunde is approved:

_____

_____

_____

Committee Chairperson

University of California, Riverside

Acknowledgments

To Dr. Seema Tiwari-Woodruff: Thank you so much for supporting and mentoring me.

To Dr. Zagha and Dr. Brown: thank you for being part of my committee.

To the Tiwari-Woodruff lab: Thank you all for your care and for allowing me to learn from you.

Dedication

To my Family

ABSTRACT OF THE THESIS

Purkinje Neuron Dysfunction in a Mouse Model of Multiple Sclerosis

by

Marvellous Erhunmwunse Osunde

Master of Science, Graduate Program in Biomedical Sciences
University of California, Riverside, June 2022
Dr. Seema Tiwari-Woodruff. Chairperson

Multiple sclerosis (MS) is a demyelinating, autoimmune, degenerative disease of the central nervous system (CNS). About 80% of MS patients have cerebellar symptoms consisting of tremors, impaired motor control, and coordination. Major aspects of Cerebellar dysfunctions are due to changes in Purkinje neurons. There is a critical need to elucidate the pathophysiology and mechanism of these symptoms. To understand this pathophysiology, we focused on energy production changes in demyelinated and damaged axons. This was achieved by investigating the role and changes in mitochondria activity of Purkinje cells in the cerebellum of an animal model of MS, experimental autoimmune encephalomyelitis (EAE). This model recapitulates axon demyelination, inflammation, and neurodegeneration of the CNS, as seen in MS. I hypothesize an increase in mitochondrial dysfunction plays a significant role in cerebellar pathology. To test this hypothesis, we conducted a longitudinal EAE cerebellum study. Cerebellar brain sections from EAE mice 21, 40, and 60 days post-induction were immunostained with myelin basic protein (MBP) and microglia specific (Iba-1), purkinje cells specific (calbindin) antibodies. Mitochondria activity in the molecular layer and Purkinje cell layer was also investigated by staining with Cytochrome Oxidase Subunit IV antibody

(CoxIV). CoxIV catalyzes the final step in the mitochondrial electron transfer chain and is regarded as one of the significant regulation sites for oxidative phosphorylation. On Day 21, after peak EAE disease, there was a decrease in MBP expression, an increase in Iba-1, and a trend with increased COXIV expression. Day 40 of EAE showed decreased MBP and increased COXIV activity compared to normal, and Day 60 EAE showed decreased MBP and increased Iba-1 with no difference in COXIV activity compared to normal. We also conducted electron microscopy on EAE Day 40 Purkinje axons to investigate axon damage and mitochondrial morphology, which showed increased axonal damage and changes to mitochondria morphology. These data demonstrate mitochondria dysfunction at peak disease following irreversible axon damage.

Table of Contents

List of Figures

List of Table

Chapter 1: Introduction

Mitochondrial Overview

The mitochondrion is a vital organelle involved in many roles. Mitochondria are double-membrane organelles with functional outer and inner membrane that separates the intermembrane space (Norat et al., 2020). The inner mitochondrial membrane encloses the mitochondrial matrix where the electron transport chain (complex I-IV) and ATP synthase are located. Both components are necessary for forming the proton gradients that drive the formation of Adenosine Triphosphate (ATP). This process is referred to as oxidative phosphorylation. Among the four complexes, complex IV (cytochrome c oxidase IV) is the terminal complex essential because of its vital role in the assembly of water molecules and respiratory functions(Y. Li, Park, Deng, & Bai, 2006). ATP is responsible for the energy used in the metabolic process for cellular function (Ahmad, Wolberg, & Kahwaji, 2018). Mitochondria play additional roles, including regulating oxidative stress and Ca2+ homeostasis. Mitochondria are highly dynamic organelles that undergo fission controlled by DRP-1 and fusion regulated by 2 GTPases optic atrophy-1 (OPA1) and mitofusin-1/2 (Mfn1/Mfn2)(Yin, Boveris, & Cadenas, 2014). Most of the time, the number of mitochondria per cell reflects the cell's energy demand. Energy-demanding tissues like muscles and neurons tend to have higher energy demands (Simcox & Reeve, 2016).

Cerebellum

The cerebellum is a significant structure in the CNS for the control of voluntary motion. The cerebellum coordinates balance, equilibrium movements, and motor

learning. It comprises two hemispheres joined by the vermis and is divided into three different lobes- anterior, posterior, and flocculonodular- separated by two fissures – primary and posterior. The primary fissure separates the anterior and posterior, and the posterior lateral fissure separates the posterior and flocculonodular lobes. The cerebellar is composed of gray matter (cerebellar cortex) and surrounding inner white matter known as the arbor vitae (tree of life). The gray matter comprises unmyelinated cell bodies and dendrites. It is subdivided into three layers – external, the molecular, the middle Purkinje cell, and the internal granular layer. The component structure of the cerebellum is essential for neuron sharpening.

Purkinje Cell

Purkinje cells (PC) are a collection of Gamma-aminobutyric acid GABAergic neurons that begin as a set of precursor cells in the cerebellar nuclei that migrate to the cortex. Their dendrites reach into the molecular layer and have multiple branches that compute thousands of signals. The elaborate dendritic structure of the PC is directly innervated by climbing fibers that come from the inferior olives of the brainstem. They release excitatory Neurotransmitters on PC, which activate PC action potential that release inhibitory NTs on Deep Cerebellar Nuclei. PCs also indirectly receive excitatory input from mossy fibers that extend their axons to golgi and granular cells. GCs send their parallel fibers to the molecular layer, which innervates the pc fibers and stimulates them. PC axons are long and pass through the granular layer into the white matter, where they are myelinated and terminate at the cerebellar nuclei. (Paul & Limaiem, 2021). The myelination of PCs supports PC axons and facilitates rapid saltatory conduction to the

deep cerebellar nuclei. Neurons like Purkinje neurons are dependent on mitochondrial oxidative phosphorylation to fulfill these energy demands due to the extensive excitatory inputs they receive from the innervated fibers (Yin et al., 2014).

Cerebellum dysfunction and related diseases

Different diseases are associated with the cerebellum and pc loss. Damage to the cerebellum and its connections results in ataxia. Ataxia describes poor muscle control that causes difficulty with movement and coordination. Some etiologies are idiopathic, traumatic, autoimmune, rare genetic disorders, and many others. Cerebellar dysfunction has been associated with neurodegenerative diseases such as Parkinson's disease (PD), Alzheimer's Disease (AD) – dementia, Huntington's Disease (HD), and Multiple Sclerosis (MS) (Samson & Claassen, 2017). PC loss is characterized as irreversible; therefore, designing therapeutics geared towards neuroprotection is vital to perverse cerebellar function (Redondo et al., 2015). HD is not associated with widespread cerebellum atrophy, but localized changes and altered connectivity are commonly reported. In AD is loss of gray and white matter, which significantly impact the connectivity of the cerebral cortex and the cerebellum. In MS, the cerebellar peduncles are common sites for lesions, and demyelination commonly occurs in cerebellar white matter (Wilkins, 2017).

MS definition

Multiple Sclerosis MS is an autoimmune, demyelinating, inflammatory disease of the central nervous system (CNS). According to the WHO update reports in 2013, about 2.3 million worldwide are estimated to have MS (Browne et al., 2014). MS affects people from 20-50 years, and studies show that females are of higher percentage to be presented with the disease. Many subtypes of MS occur as relapsing or progressive in patients. MS, as a diverse neurological condition, affects areas of abundant white matter, including the corpus callosum, cerebellum, and spinal cord. It is characterized as inflammatory demyelination and is followed by axon damage (Kurtzke, Beebe, Nagler, Kurland, & Auth, 1977). MS patients may present with acute cerebellar dysfunction, associated with acute relapse or chronic cerebellar disorders in progressive disease (Wilkins, 2017). Approximately 80% of MS patients present with cerebellar symptoms, which are prevalent in progressive disease. (Kutzelnigg et al., 2007). Previous studies have shown that cerebellar cortical is substantially demyelinated and is a potential substrate of cerebellar dysfunction in MS (Kutzelnigg et al., 2007). In studying the pathophysiology of MS in the context of cerebellar dysfunction, our lab and others have shown that Purkinje cell loss is prevalent within cerebellar lesions (Kutzelnigg et al., 2007). Overall, the involvement of the cerebellum at the onset of the disease is also reported to worsen prognosis, thus the importance of understanding the pathophysiology of the cerebellum (Weinshenker et al., 1991).

With the complexity of the MS, a specific cause for the pathogenesis is yet to be identified. Using post-mortem tissue can sometimes be difficult due to the one time-point

window to study pathology, the clinical signs and symptoms variability among MS patients difficult. As a result of the limitations of post-mortem studies, there is a need for an animal model able to recapitulate MS.

We used experimental autoimmune encephalomyelitis EAE to study Purkinje cell loss and mitochondrial dysfunction. This animal model of MS recapitulates inflammation, demyelination, and neurodegeneration (Hasselmann, Karim, Khalaj, Ghosh, & Tiwari-Woodruff, 2017). It uses a myelin peptide to induce an autoimmune reaction throughout the brain and spinal cord. However, variation in the cohorts occurs because the lesions formed can develop anywhere in the CNS. A study conducted by (MacKenzie-Graham et al., 2009) showed that cerebellar gray matter atrophy was regionally specific in using the EAE model of MS. Further studies showed increased inflammation, demyelination, and pc loss.

Demyelination can directly affect mitochondria dynamics due to changes in fission and fusion (Ohno et al., 2014). Fission and fusion are critical to mitochondria because they affect mitochondria morphology and distribution within the cell. Drp1 has been effectively studied in the EAE mouse model. Luo et al. observed increased Drp1 expression in the lesioned spinal cord at peak EAE disease and corpus callosum after six weeks on the CPZ diet (F. Luo, K. Herrup, X. Qi, & Y. Yang, 2017; Fucheng Luo, Karl Herrup, Xin Qi, & Yan Yang, 2017). Hyperactivation of Drp1 in culture contributed to an increase in mitochondrial fission; however, inhibiting Drp1 activation had a neuroprotective effect in both EAE and CPZ (Fucheng Luo et al., 2017). Direct manipulation of mitochondrial proteins by deleting SLC25A46, an OMM protein,

showed degenerating dendrites, enlarged mitochondria in Purkinje cells, and decreased ATP production compared to controls (Z. Li et al., 2017). In addition, there was an increase in Mfn2 expression in PLP4e mice, a demyelinating mouse model containing extra copies of myelin genes (Thai et al., 2019). While these studies show direct changes in mitochondria, these changes are only observed after a protein is knocked out or after extra copies of genes are added. Due to genetic alterations, these studies cannot translate to human disease and post-mortem tissue. Studies also showed decreased mitochondrial complex expression in EAE after depletion of LKB1 from astrocytes (Kalinin et al., 2020). These findings provide why it is crucial to elucidate the PC mitochondrial dysfunction in cerebellar symptoms of MS.

General Methodology

Animals

This study followed the protocol established by the American Veterinary Medicine in accordance with the National Institute of Health (NIH) and were approved by the Institutional Animal Care and Use Committee (IACUC) at UCR, Riverside. Eight-week-old C57BL/6 male mice were obtained from Jackson Laboratory and maintained in-house at the animal facility. Animals were held at five per cage with standard light/dark cycles.

Animal groups

Mice were categorized into three groups Normal, EAE induced mice treated with vehicle and Estrogen receptor ligand - O-methyl. EAE mice cerebellums were perfused, isolated,

and use for immunohistochemistry on days 21-24, with treatment starting on day 17 after clinical score scores showed the severity of the disease.

Experimental Autoimmune Encephalomyelitis EAE

Active EAE was induced in eight-week-old female Thy1-YFP mice as previously described (Hasselmann et al., 2017). Briefly, mice received two subcutaneous (s.c) injections, each consisting of MOG_{35-55} peptide (Mimotopes, Clayton, Victoria, Australia) emulsified with M. butyricum-containing complete Freund's adjuvant (BD Difco, Franklin Lakes, NJ) supplemented with M. tuberculosis (BD Difco), followed by two intraperitoneal injections of Bordetella pertussis toxin (List Biological Laboratories, Campbell, CA). Mice were monitored daily according to a standard EAE clinical disease scoring scale ranging from 0-to 5.

Immunohistochemistry

Mice were transcardially perfused with 1x PBS followed by fixation of the tissues using 10% formalin. Tissues were cryoprotected in 30% sucrose and later embedded in gelatin for sectioning. The embedded brains were cut into 40um sagittal sections and were stored in PBS with 1% sodium azide at 4 degrees, ready to be used for IHC analysis.

IHC analysis used a permeabilization buffer of 0.3% Triton X-100 and a blocking buffer of 15% normal goat serum NGS. The following antibodies were used: chicken anti-myelin basic protein (MBP; AB9348, polyclonal, EMD Millipore, Darmstadt, Germany), rabbit anti-Iba1 (Iba-1; 019-19741, polyclonal, Wako), Calbindin (C9848-2ml) and COXIV (Novus; NB110-39115). Secondary staining was performed using polyclonal fluorophore-conjugated antibodies: goat anti-chicken Alexa Fluor cy3, goat anti- rabbit

Invitrogen 647 (Thermo fisher scientific), and goat anti-mouse Invitrogen 555 (Thermo Fisher Scientific) were used. Nuclei were counter-stained with 4', 6-Diamidino-2-phenylindole (DAPI, two ng/ml: Molecular Probes) for 10 minutes after incubation with secondary antibodies. Tissue sections were mounted on glass slides, allowed to dry for about an hour, and coverslipped with Fluoromount G mounting medium (Thermo Fisher Scientific) for imaging.

Table of antibodies used

ANTIBODY NAME	**SOURCE**	**Vendor**	**LOT**	**CATALOG**	**Isotype**
MBP	Chicken		3284364	AB9348	
IBA1	Rabbit-Poly	FUJIFILM Wako	LEJ1842	019-19741	IgG
Calbindin	MS-Mono	SIGMA	0000118423	C9848-2ML	IgG1
COX IV	Rb-Poly	NOVUS	D-3	NB110-39115	IgG

Quantification and Microscopy

Image analysis was conducted using an Olympus BX61 confocal microscope (Olympus America Inc., Center Valley, PA) with z-stack projections performed using slidebook6. Counts and analyses of the cerebellar cortex were performed blindly using ImageJ (NIH, Bethesda, MD). Puncta analysis in the COXIV images was adapted from (Horzum, Ozdil, & Pesen-Okvur, 2014). The background was subtracted, and the CLAHE and Math> Exp were used.

Electron Microscopy (EM)

Cerebellums were post-fixed in 2% glutaraldehyde and 5% formalin for 24hr. They were processed for EM, imaged, and photographed. The g-ratio(the ratio of axon diameter to the total myelinated fiber diameter) and the number of myelinated and unmyelinated axons were quantified for at least 200 per Normal and EAE D40. N=5. For each axon, two diameter measurements were taken and averaged out.

Statistics

Statistical analyses were performed using Prism® (GraphPad, La Jolla) program for Windows. There were 4-5 mice per treatment group. For IHC, two sections per mouse were taken for the cerebellum. Graph values are expressed as mean $\pm$ standard error of the mean. For histology, and *in vivo* studies, statistical analysis of mean values was carried out using one-way ANOVA if mean values passed a normality test or Kruskal Wallis multiple comparison test if they did not. Differences were considered significant at the *$p<0.05$, **$p<0.01$, ***$p<0.001$, and ****$p<0.0001$ level

Results

EAE mice show demyelination and inflammation

To assess changes in demyelination and inflammation, granule cell layer (GCL) and white matter (WM) of longitudinal cerebellar sections were evaluated using IHC. The GCL is where Purkinje cells and climbing axons are located, and the WM is where all of the axons of the cerebellar cortex exit towards the cerebellar peduncles (**Figure 1A**). Myelin basic protein (MBP) expression throughout the white matter and cerebellar

peduncles in the EAE mice showed a visual decrease compared to the normal mice, especially in the chronic EAE mice (**Figure 1A**). 20x images taken of lobule IV looking at the GCL and WM layers showed a significant decrease in MBP expression in both layers in the EAE mice compared to the normal, beginning at peak EAE disease (EAE D21) and persisting through chronic EAE (EAE D40 and EAE D60) (**Figure 1B, C**).

To assess inflammation in the cerebellum after EAE induction, we used ionized calcium-binding adaptor molecule 1 (Iba1), a marker for microglia and macrophages. There was an increase in Iba1 expression in both the GCL and WM in the EAE mice compared to the normal mice at EAE D40 and EAE D60 (**Figure 1D, E**).

EAE mice show an increase in Purkinje Cell loss

To assess Purkinje cell loss, we used calbindin as a biomarker for PC cell bodies and dendrites. Calbindin is a calcium-binding protein belonging to the troponin C superfamily. It is expressed in Purkinje cells and is an essential determinant of motor coordination and sensory integration. 10x images were taken at lobule IV, counting Purkinje soma. There was a decrease in Calbindin + positive cells in EAE mice compared to the normal mice across time points (**Figure 2**).

EAE mice and mitochondria activity

To analyze the protein expression of mitochondria in EAE mice, we used CoxIV as a biomarker. Cytochrome C Oxidase (COX) hetero-oligomeric enzyme subunit IV (CoxIV) is the last component of the electron transport chain before ATP synthase. It is frequently used as a marker for mitochondria activity (**Figure 3A**). This catalyzes the reduction of oxygen to water. CoxIV receives an electron from each of four cytochrome c

molecules and transfers them to one dioxygen molecule, converting molecular oxygen to 2 molecules of water. This marker is located on the inner mitochondrial membrane and is generally upregulated when mitochondrial demand is increased. As a result, we observed a significant decrease in CoxIV staining in EAE mice compared to the normal mice at EAE D40 and EAE D60 (**Figure 3B**).

EAE mice and axon size Electron microscopy

To further characterize Mitochondrial dynamics and axon damage Electron Microscopy (EM) was performed. (**Figure 4B**). EM is a technique used for obtaining high-resolution images of biological and non-biological specimens. It investigates the detailed structure of tissues, cells, organelles, and macromolecular complexes. Interestingly EM analysis showed changes in mitochondria morphology where there was an increase in mitochondria size at EAE D40 compared to normal. (**Figure 4C**).

To assess Purkinje axon myelination integrity, ultrastructure EM analysis of Purkinje axons cross-sections from different groups was performed. Within a given field, myelinated axons and non-myelinated axons were assessed for the mean ratio of the inner axon diameter to the total outer diameter (G-ratio) (**Figure 4D**). EAE sections revealed an increase in demyelinated axons and higher g-ratios compared to normal.

Discussion

in this present study, MOG-EAE was used to investigate MS-related mitochondrial dysfunction Purkinje neuron pathology. Mice induced with EAE were assessed for mitochondria and Purkinje cell functionality, morphology, and pathology in the disease. This study was done longitudinally at peak disease D21 and last onset of D40 and D60 to assess different time points of disease progression. Our results show that EAE causes functional deficit on PC, including inflammation, demyelination, and axon damage, and is a good mouse model for studying Multiple Sclerosis. We can also show that mitochondrial activity is affected by the disease, which in turn might be the major cause of PC dysfunction.

Approximately 80% of MS patients experience a worse prognosis associated with cerebellar symptoms (Kutzelnigg et al., 2007). This is of no doubt to note since the cerebellum comprises Purkinje neurons as the sole output of the cerebellum and is heavily myelinated. Due to the size of PCs, they require high metabolic recourses to expend and be able to carry our functional activity. PC neurons depend on mitochondrial oxidative phosphorylation to meet energy demands.

Immunohistochemistry (IHC) is used for most post-mortem studies to indicate mitochondrial involvement during multiple sclerosis. In chronic active MS lesions, one study observed increased mitochondria content (measured by porin) compared with myelinated axons. However, there was no difference in axonal mitochondrial content between remyelinated and demyelinated axons in remyelinated regions close to demyelinated areas in chronic MS lesions (Zambonin et al., 2011). In addition, a reduction in mitochondrial content was observed in shadow plaques compared with

chronically demyelinated axons in MS lesions (Zambonin et al., 2011). Using IHC methods to study mitochondria activity, we measured CoxIV activity. This is because of its involvement with the ETC and its ability to catalyze oxygen reduction to water. This marker is located on the inner mitochondrial membrane and is generally upregulated when mitochondrial demand is increased.

Previous studies have shown that in several models of EAE, the cerebellum is targeted. Using the MOG 33-55 AA model, we were able to show and demonstrate demyelination, inflammation, and axon damage (Hasselmann et al., 2017; Karim et al., 2019; MacKenzie-Graham et al., 2009). Demyelination in the cerebellum has been observed as early as D14 through to D55, which is consistent with our data. With inflammation, we know that EAE is t- cell-mediated activating peripheral immune response leading to pro-inflammation. Macrophages and T-cells infiltrate the CNS due to a compromised blood-brain barrier and release a combination of proinflammatory cytokines contributing to inflammation (Constantinescu, Farooqi, O'Brien, & Gran, 2011). In the CNS, microglia comprise about 10% of the total number of cells. Our data showed the increased activation of microglia/macrophages in EAE mice using the biomarker iba-1, which is concurrent with other studies (Chu et al., 2018). With inflammatory segmental demyelination giving rise to axon damage, there are other factors that might be responsible for axon damage. Some studies have shown focal axon damage that is present before demyelination may be due to macrophages-derived reactive oxygen and nitrogen species (ROS and NOS) (Nikic et al., 2011). The association of ROS or NOS can further trigger mitochondrial pathology.

With studies showing the relation between mitochondria pathology and axon damage, we first looked at PC cell protein expression and morphology using IHC and Electron Microscopy. We observed a decrease in calbindin+ cells as the disease progressed. We suspect that not only are demyelination and inflammation responsible for the cell loss but changes in mitochondrial activity and morphology. We believe that disruption to mitochondrial dynamics contributes to PC loss.

In summary, we have demonstrated that mitochondrial dysfunction is a major cause of Purkinje cell pathology during autoimmune-mediated demyelination. Understanding the relationship between these will allow for therapeutic designs that target mitochondria dynamics and allow for further cell type-specific studies.

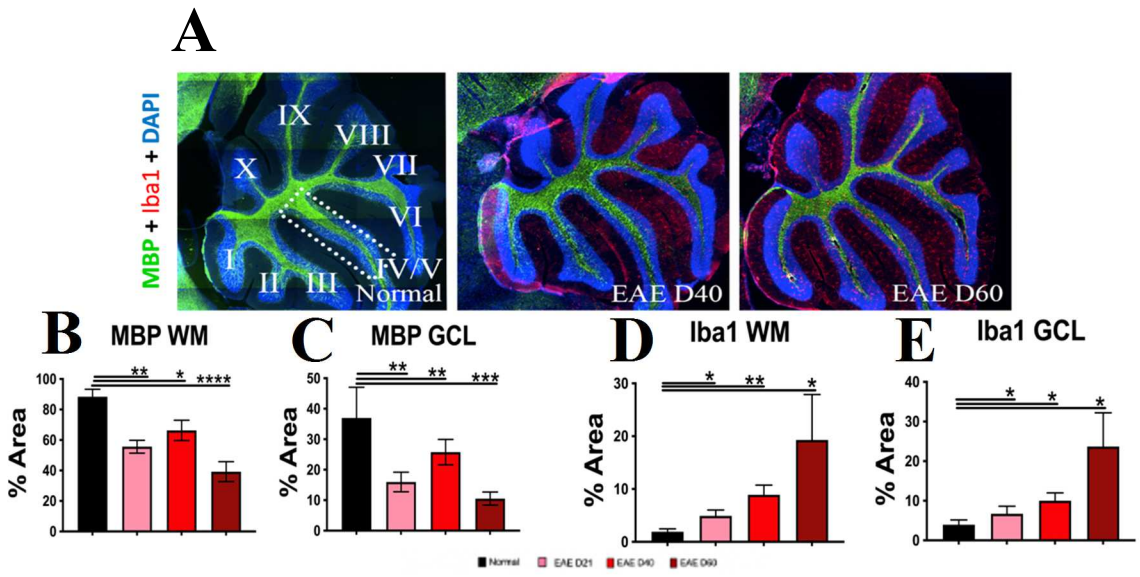

Figure 1: EAE mice have demyelination and inflammation in the cerebellum's granule cell layer and white matter. (A) 10X montages displaying sagittal sections of myelin basic protein (MBP; green) + ionized calcium-binding adaptor molecule 1 (Iba1; Red) + 4',6-diamidino-2-phenylindole (DAPI; blue). Representative montage of EAE D40 and EAE D60 shows a decrease in MBP staining intensity with an increase in Iba1 staining intensity as compared to Normal **(B)** MBP WM analysis showed a decrease in MBP expression at EAE D21, EAE D40, and EAE D60 compared to normal, **(C)** which is also shown in the GCL. **(D)** There is an increase in Iba1 expression in the WM **(E** and GCL at EAE D21, EAE D40, and EAE D60 compared to normal. Normal: n=10, EAE D21: n=10, EAE D40: n=10, EAE D60: n=10. Data are represented as mean ± SEM. *p < .05, **** p <.0001. Scale bar: 100µm.

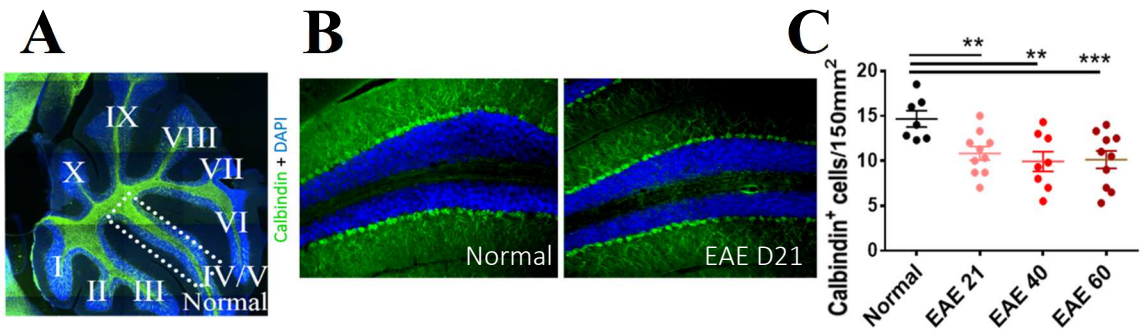

Figure 2: EAE mice depict Purkinje cell loss in the cerebellum. (A) 10X montage displaying sagittal section of myelin basic protein (MBP; green) + 4',6-diamidino-2-phenylindole (DAPI; blue). **(B)** Representative 20X images from lobule IV/V immunostained with Calbindin and DAPI to quantify Purkinje cell counts in the gray matter **(C)** Calbindin analysis showed a decrease in calbindin $^{+}$ cells at EAE D21, EAE D40. EAE D60 compared to normal, Normal: n=10, EAE D21: n=10, EAE D40: n=10, EAE D60: n=10. Data are represented as mean $\pm$ SEM. *p < .05, **** p <.0001. Scale bar: 100µm.

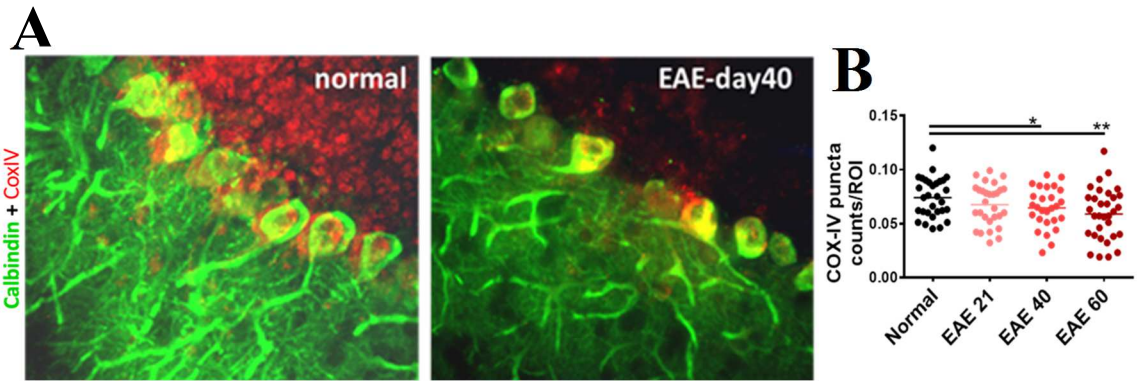

Figure 3: EAE mice have decreased mitochondrial activity. (A) Representative 40X images from lobule IV/V immunostained with Calbindin and COXIV to quantify Purkinje cell counts and Mitochondria activity in the gray matter**) (B)** COXIV analysis showed a decrease in COXIV puncta at EAE D40, and EAE D60 compared to normal, Normal: n=10, EAE D21: n=10, EAE D40: n=10, EAE D60: n=10. Data are represented as mean ± SEM. *p < .05, **** p <.0001. Scale bar: 100µm.

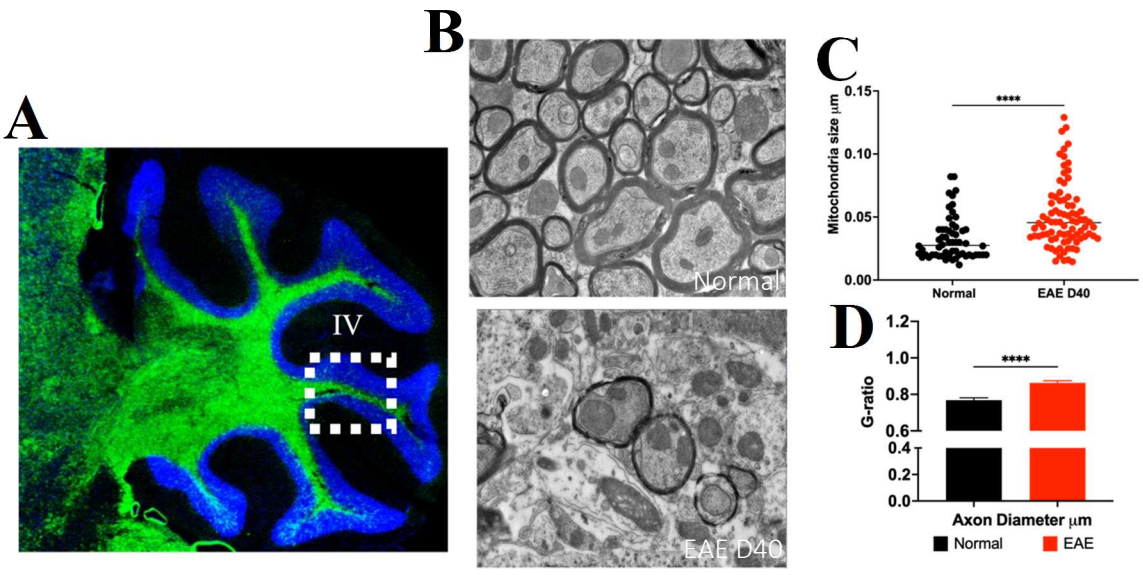

Figure 4: EAE mice have alternations in mitochondria size and PC axons. (A) 10X montages displaying sagittal sections of myelin basic protein (MBP; green) + 4',6-diamidino-2-phenylindole (DAPI; blue). **(B)** Cerebellums from normal, and EAE D40 mice were collected and prepared for EM to assess individual PC axons. Cross-sectioned cerebellum micrographs reveal coherent myelinated axons in normal mice. EAE D40 mice show significant damage to axons and demyelination **(C).** Quantifying the number of axons with changes in mitochondrial morphology showed an increase in mitochondrial size with EAE D40 mice compared to normal mice. **(D)** Calculated g-ratios are significantly increased in EAE D40 mice compared to normal n=4-5 mice per group. Data are represented as mean $\pm$ SEM. *p < .05, **** p <.0001. Scale bar: 100µm for A and 0.1µm for E.

References

Ahmad, M., Wolberg, A., & Kahwaji, C. I. (2018). Biochemistry, electron transport chain.

Barcelos, I. P. d., Troxell, R. M., & Graves, J. S. (2019). Mitochondrial dysfunction and multiple sclerosis. *Biology, 8*(2), 37.

Browne, P., Chandraratna, D., Angood, C., Tremlett, H., Baker, C., Taylor, B. V., & Thompson, A. J. (2014). Atlas of Multiple Sclerosis 2013: A growing global problem with widespread inequity. *Neurology, 83*(11), 1022-1024.

Chu, F., Shi, M., Zheng, C., Shen, D., Zhu, J., Zheng, X., & Cui, L. (2018). The roles of macrophages and microglia in multiple sclerosis and experimental autoimmune encephalomyelitis. *Journal of neuroimmunology, 318*, 1-7.

Constantinescu, C. S., Farooqi, N., O'Brien, K., & Gran, B. (2011). Experimental autoimmune encephalomyelitis (EAE) as a model for multiple sclerosis (MS). *British journal of pharmacology, 164*(4), 1079-1106.

Dutta, R., McDonough, J., Yin, X. G., Peterson, J., Chang, A., Torres, T., . . . Trapp, B. D. (2006). Mitochondrial dysfunction as a cause of axonal degeneration in multiple sclerosis patients. *Annals of Neurology, 59*(3), 478-489. doi:10.1002/ana.20736

Hasselmann, J. P. C., Karim, H., Khalaj, A. J., Ghosh, S., & Tiwari-Woodruff, S. K. (2017). Consistent induction of chronic experimental autoimmune encephalomyelitis in C57BL/6 mice for the longitudinal study of pathology and repair. *Journal of Neuroscience Methods, 284*, 71-84. doi:10.1016/j.jneumeth.2017.04.003

Horzum, U., Ozdil, B., & Pesen-Okvur, D. (2014). Step-by-step quantitative analysis of focal adhesions. *MethodsX, 1*, 56-59.

Kalinin, S., Meares, G. P., Lin, S. X., Pietruczyk, E. A., Saher, G., Spieth, L., . . . Benveniste, E. N. (2020). Liver kinase B1 depletion from astrocytes worsens disease in a mouse model of multiple sclerosis. *Glia, 68*(3), 600-616.

Karim, H., Kim, S. H., Lauderdale, K., Lapato, A. S., Atkinson, K., Yasui, N., . . . Tiwari-Woodruff, S. K. (2019). Analogues of ERβ ligand chloroindazole exert immunomodulatory and remyelinating effects in a mouse model of multiple sclerosis. *Scientific Reports, 9*(1), 503.

Kurtzke, J. F., Beebe, G. W., Nagler, B., Kurland, L. T., & Auth, T. L. (1977). Studies on the natural history of multiple sclerosis—8: early prognostic features of the later course of the illness. *Journal of chronic diseases, 30*(12), 819-830.

Kutzelnigg, A., Faber□Rod, J. C., Bauer, J., Lucchinetti, C. F., Sorensen, P. S., Laursen, H., . . . Schmidbauer, M. (2007). Widespread demyelination in the cerebellar cortex in multiple sclerosis. *Brain pathology, 17*(1), 38-44.

Li, Y., Park, J.-S., Deng, J.-H., & Bai, Y. (2006). Cytochrome c oxidase subunit IV is essential for assembly and respiratory function of the enzyme complex. *Journal of bioenergetics and biomembranes, 38*(5), 283-291.

Li, Z., Peng, Y., Hufnagel, R. B., Hu, Y.-C., Zhao, C., Queme, L. F., . . . Lu, Q. R. (2017). Loss of SLC25A46 causes neurodegeneration by affecting mitochondrial dynamics and energy production in mice. *Human molecular genetics, 26*(19), 3776-3791.

Luo, F., Herrup, K., Qi, X., & Yang, Y. (2017). Inhibition of Drp1 hyper-activation is protective in animal models of experimental multiple sclerosis. *Exp Neurol, 292*, 21-34. doi:10.1016/j.expneurol.2017.02.015

Luo, F., Herrup, K., Qi, X., & Yang, Y. (2017). Inhibition of Drp1 hyper-activation is protective in animal models of experimental multiple sclerosis. *Experimental neurology, 292*, 21-34.

MacKenzie-Graham, A., Tiwari-Woodruff, S. K., Sharma, G., Aguilar, C., Vo, K. T., Strickland, L. V., . . . Jacobs, R. E. (2009). Purkinje cell loss in experimental autoimmune encephalomyelitis. *Neuroimage, 48*(4), 637-651.

Nikic, I., Merkler, D., Sorbara, C., Brinkoetter, M., Kreutzfeldt, M., Bareyre, F. M., . . . Kerschensteiner, M. (2011). A reversible form of axon damage in experimental autoimmune encephalomyelitis and multiple sclerosis. *Nature Medicine, 17*(4), 495-U135. doi:10.1038/nm.2324

Norat, P., Soldozy, S., Sokolowski, J. D., Gorick, C. M., Kumar, J. S., Chae, Y., . . . Levitt, M. R. (2020). Mitochondrial dysfunction in neurological disorders: Exploring mitochondrial transplantation. *NPJ Regenerative medicine, 5*(1), 1-9.

Ohno, N., Chiang, H., Mahad, D. J., Kidd, G. J., Liu, L. P., Ransohoff, R. M., . . . Trapp, B. D. (2014). Mitochondrial immobilization mediated by syntaphilin facilitates survival of demyelinated axons. *Proceedings of the National Academy of Sciences of the United States of America, 111*(27), 9953-9958. doi:10.1073/pnas.1401155111

Paul, M. S., & Limaiem, F. (2021). Histology, Purkinje Cells. In *StatPearls [Internet]*: StatPearls Publishing.

Redondo, J., Kemp, K., Hares, K., Rice, C., Scolding, N., & Wilkins, A. (2015). Purkinje cell pathology and loss in multiple sclerosis cerebellum. *Brain Pathology, 25*(6), 692-700.

Rose, J., Brian, C., Woods, J., Pappa, A., Panayiotidis, M. I., Powers, R., & Franco, R. (2017). Mitochondrial dysfunction in glial cells: Implications for neuronal homeostasis and survival. *Toxicology, 391*, 109-115.

Sadeghian, M., Mastrolia, V., Haddad, A. R., Mosley, A., Mullali, G., Schiza, D., . . . Smith, K. J. (2016). Mitochondrial dysfunction is an important cause of neurological deficits in an inflammatory model of multiple sclerosis. *Scientific Reports, 6*, 14. doi:10.1038/srep33249

Samson, M., & Claassen, D. O. (2017). Neurodegeneration and the cerebellum. *Neurodegenerative Diseases, 17*(4-5), 155-165.

Simcox, E. M., & Reeve, A. K. (2016). An introduction to mitochondria, their structure and functions. In *Mitochondrial Dysfunction in Neurodegenerative Disorders* (pp. 3-30): Springer.

Simkins, T. J., Duncan, G. J., & Bourdette, D. (2021). Chronic demyelination and axonal degeneration in multiple sclerosis: pathogenesis and therapeutic implications. *Current neurology and neuroscience reports, 21*(6), 1-11.

Thai, T. Q., Nguyen, H. B., Sui, Y., Ikenaka, K., Oda, T., & Ohno, N. (2019). Interactions between mitochondria and endoplasmic reticulum in demyelinated axons. *Medical Molecular Morphology, 52*(3), 135-146.

Weinshenker, B. G., Rice, G., Noseworthy, J., Carriere, W., Baskerville, J., & Ebers, G. (1991). The natural history of multiple sclerosis: a geographically based study: 3. Multivariate analysis of predictive factors and models of outcome. *Brain, 114*(2), 1045-1056.

Wilkins, A. (2017). Cerebellar dysfunction in multiple sclerosis. *Frontiers in neurology, 8*, 312.

Yin, F., Boveris, A., & Cadenas, E. (2014). Mitochondrial energy metabolism and redox signaling in brain aging and neurodegeneration. *Antioxidants & redox signaling, 20*(2), 353-371.

Zambonin, J. L., Zhao, C., Ohno, N., Campbell, G. R., Engeham, S., Ziabreva, I., . . . Mahad, D. J. (2011). Increased mitochondrial content in remyelinated axons: implications for multiple sclerosis. *Brain, 134*, 1901-1913. doi:10.1093/brain/awr110